J. Ocean Univ. China (Oceanic and Coastal Sea Research)
https://doi.org/10.1007/s11802-025-6088-4
ISSN 1672-5182, 2025 24 (4): 1111-1120
http://www.ouc.edu.cn/xbywb/
E-mail:xbywb@ouc.edu.cn

An Aminosugar-Rich Heteropolysaccharide Isolated from *Sepia esculenta* Ink

JI Cheng, XIA Zefeng, NIU Chunyu, CHEN Yan, PEI Jinfeng*, and CHEN Yin*

College of Food and Pharmacy, *Zhejiang Ocean University*, *Zhoushan* 316022, *China*

(Received November 30, 2024; revised February 24, 2025; accepted March 28, 2025)

Abstract The polysaccharides from *Sepia esculenta* ink are potential candidates for biomedical applications due to their functional properties. In our study, a heteropolysaccharide, SE-1, isolated from *Sepia esculenta* ink, had a molecular weight of 13.1 kDa and a monosaccharide composition of Man:GlcN:GlcUA:GalN:Xyl:Fuc=1.00:1.38:0.65:2.89:0.76:1.99. Through partial acid hydrolysis, methylation and one- and two-dimensional nuclear magnetic resonance (1D and 2D NMR) spectroscopic analyses, it is indicated that the structure of SE-1 consists of →4)-α-D-Glc*p*NAc-(1→, →4)-α-L-Fuc*p*-(1→, →3)-α-D-Gal*p*NAc-(1→, →2,6)-α-D-Man*p*-(1→ and →3)-β-D-Glc*p*UA-(1→ as the main chain and single terminal β-D-Xyl*p*-(1→, which links to *O*-2 of (1→2,6)-α-Man*p*, as the side chain. A new aminosugar-abundant heteropolysaccharide was isolated from *S. esculenta* ink for the first time.

Key words *Sepia esculenta* ink; separation and purification; structure determination; heteropolysaccharide

1 Introduction

Squid ink, a substance extracted from the ink sacs of animals in the squid family, is named according to its color and origin. Fresh squid ink is a viscous suspension containing fine black pigment particles along with water, proteins, polysaccharides, and lipids (Li *et al*., 2004). Squid ink polysaccharides (SIPs), which are significant bioactive compounds derived from squid ink, belong to the glycosaminoglycan class. Research revealed that peptidoglycans isolated from squid ink exhibit potent inhibitory effects on sarcoma cell growth, highlighting the potential of squid ink in medicinal research (Takaya *et al*., 1994). Further studies identified that SIP from Argentine squid contained equal molar of glucuronic acid (GlcUA), N-acetylgalactosamine (GalNAc) and fucose (Fuc) (Takaya *et al*., 1996). Recent investigations have shown that SIPs from different sources displayed a range of biological activities, including antitumor, antioxidant, anticoagulant, and immunomodulatory effects.

SIP primarily exerted its antitumor effects through several mechanisms, including the induction of apoptosis in tumor cells (Zhang *et al*., 2015), inhibition of tumor angiogenesis (Schmitt *et al*., 2012; Patan, 2014; Hide *et al*., 2016), and resistance to tumor invasion and metastasis (Jeong *et al*., 2014; Clark *et al*., 2015; Jin *et al*., 2016). In the case of the human ovarian cancer cell line SKOV-3, SIP treatment has shown to inhibit the expression of the intracellular protein epidermal growth factor receptor (EGFR) and indirectly reduce epidermal growth factor (EGF) activity by binding to EGFR, thereby diminishing the metastasis and invasion capabilities of SKOV-3 cells (Jiang *et al*., 2018). Furthermore, SIP up-regulates the expression levels of pro-apoptotic proteins in SKOV-3 cells and significantly inhibits the expression of poly (ADP-ribose) polymerase-1 (PARP-1), leading to apoptosis induction (Zong *et al*., 2013). Studies had also highlighted SIP's strong total antioxidant capacity, demonstrating effective scavenging of DPPH (1,1-Diphenyl-2-picrylhydrazyl) radicals, hydroxyl radicals (-OH), and its ability to repair H_2O_2-induced damage (Luo and Liu, 2013). SIP enhanced the activities of superoxide dismutase (SOD) and catalase (CAT), reduced malondialdehyde levels, and protected mitochondrial function (Gu *et al*., 2017). Additionally, SIP maintained the REDOX balance in mouse testis by activating the Nrf2 pathway, which enhanced the activity of downstream antioxidant and phase II detoxification enzymes (Le *et al*., 2015). In terms of neuroprotection, SIP reduced the release of LDH from PC12 cells induced by 6-OHDA, significantly increased SOD activity, and decreased malondialdehyde (MDA) levels (Ye *et al*., 2019). Moreover, SIP and its derivatives could prolong partial thromboplastin time (PTT) and prothrombin time (PT), indicating their anticoagulant effects through the inhibition of both endogenous and exogenous clotting processes. S-SIP, a derivative of SIP, achieved anticoagulant effects by inhibiting the expressions of coagulation factors FIIa and FXa (Li *et al*., 2018). The primary components of SIP and its derivatives elevated antithrombin III

* Corresponding authors. E-mail: pffzjut@163.com
E-mail: mojojo1984@163.com

(AT-III) levels in normal mice, which subsequently prolonged clotting time. In chemotherapy mice, levels of clotting factors II (FII), X (FX), and AT-III were significantly improved (Li *et al*., 2022). SIP and its derivatives also enhanced both specific and non-specific immunity by increasing immune cell counts and regulating cytokine production. SIP up-regulated the mRNA and protein expression levels of compact linking proteins such as claudin-2 and cingulin, thereby enhancing the immune function of gastrointestinal epithelial cells (Zuo *et al*., 2015). Low molecular weight SIPs (LMWSIPs) significantly promoted spleen lymphocyte proliferation in mice (Tian *et al*., 2023). Additionally, SIP exhibited significant antibacterial and preservative effects on squid stored at low temperatures (Shi *et al*., 2015).

Due to its rich pigment content, proteoglycans, and extensive biological activity, squid ink has attracted significant attention of the researchers. It has evolved from a mere by-product of cephalopod processing to a vital raw material for functional products. As a result, various sources of squid ink are now being extensively researched. *Sepia esculenta*, commonly known as cuttlefish, is particularly noteworthy due to its short growth cycle, rapid reproduction, delicious meat, rich nutritional profile, and high protein content, all of which contribute to its substantial economic and medicinal value (Liu *et al*., 2023).

Polysaccharides extracted from various cephalopod species exhibit structural variations, reflecting differences in monosaccharide composition, sulfation patterns, and glycosidic linkages. For example, polysaccharides from *Ommastrephes bartramii* ink were reported to consist mainly of glucuronic acid (GlcUA), N-acetylgalactosamine (GalNAc), and fucose (Fuc) in an approximately equimolar ratio (Ye *et al*., 2019). Similarly, *Sepiella maindroni* ink polysaccharides were found to contain Fuc, GalNAc, mannose (Man), and GlcUA in a 2:2:1:1 ratio, forming a glycosaminoglycan-like structure (Liu *et al*., 2008). These studies highlight the presence of sulfated and non-sulfated glycosaminoglycan-like polysaccharides in different squid species. However, there have been no reports of polysaccharides from *Sepia esculenta* ink before this study. Compared to known SIPs, the polysaccharide isolated in this study is distinguished by its high content of aminosugars, particularly both N-acetylglucosamine (GlcNAc) and N-acetylgalactosamine (GalNAc), along with fucose and uronic acids. This composition is different with previously studied squid ink polysaccharides, which typically contain either GlcNAc or GalNAc but not both. Additionally, SE-1 possesses a slightly branched structure. This complex architecture further differentiates it from other known SIPs. This study, therefore, provides the structural characterization of an aminosugar-rich heteropolysaccharide from *Sepia esculenta* ink for the first time, expanding the understanding of cephalopod-derived polysaccharides and their potential bioactivities. Further comparisons with other marine-derived polysaccharides, particularly those from related cephalopod species, will help elucidate structure-function relationships and contribute to the development of novel bioactive compounds from squid ink polysaccharides. As a valuable cephalopod resource, *Sepia esculenta* produces various visceral by-products, including ink sacs, during processing. This paper investigated the structural characteristics of polysaccharides derived from *Sepia esculenta* ink.

2 Materials and Methods

2.1 Materials

PC12 cell was obtained from Procell Life Science & Technology Co., Ltd. Lactate dehydrogenase (LDH), 3-(4,5-dimethylthiazol-2-yl)-2,5-diphenyltetrazolium bromide (MTT), and reactive oxygen species (ROS) cytotoxicity assay kits were purchased from Beyotime Biotechnology Co., Ltd. The remaining reagents were of analytical grade (Zhejiang Haoke Century Biotechnology Co., Ltd., Hangzhou, China).

2.2 Extraction and Purification of the Squid Ink Polysaccharide

The ink sac was harvested from the squid's viscera, and the squid ink was extracted from the sac. The extracted ink was then concentrated and freeze-dried for subsequent experiments. Polysaccharides from cuttlefish ink were obtained through the digestion of two distinct enzymes (Liu *et al*., 2022).

Cuttlefish ink was mixed with distilled water at a ratio of 1:20 (w/v) and subjected to magnetic stirring at 40 °C for 2 h to ensure uniform dispersion. The enzymatic hydrolysis included two steps. Firstly, cuttlefish ink was digested with 2% papain at 60 °C and pH 7.0 for 3 h. Then it was digested by 0.5% trypsin at 60 °C and pH 10.0 for an additional 3 h. Subsequently, the solution was heated and centrifuged to remove insoluble substances. The precipitation was removed and concentrated, then ethanol was added for alcohol precipitation and centrifugation. The supernatant was collected for dialysis (3500 Da). The crude polysaccharides were obtained after freeze-drying with a 3.0% (w/v) yielding.

The crude polysaccharide was formulated as 50 mg/mL. Following centrifugation, the supernatant was collected and processed using Q Sepharose 4 Fast Flow column chromatography (3.5 cm×30 cm) with an AKTA-FPLC fast protein purification system. The sample was eluted with 0 to 2 mol/L NaCl solutions and collected. Using phenol-sulfuric acid method (Chen *et al*., 2011), the absorbance was measured at 490 nm. The sugar distribution patterns were analyzed from this linear elution curve, enabling targeted separation using specific NaCl concentrations. Finally, the separated fractions were sequentially collected, concentrated, dialyzed, and freeze-dried (Chen *et al*., 2013).

2.3 Physicochemical Analysis and Molecular Weight Determination of the Squid Ink Polysaccharide

The total sugar, protein and aminosugar contents were determined by sulfuric acid-phenol, Folin-phenol and the Ehrlich method, respectively. The content of sulfate in the

samples was determined by ion exchange chromatography. Molecular weight was determined using high performance gel permeation chromatography (HPGPC) equipped with Shodex Ohpak SB-804HQ column (300 mm×8 mm) (Lowry *et al*., 1951; Reissig *et al*., 1955; Dubois *et al*., 1956; Zhang *et al*., 2013).

2.4 Monosaccharide Composition Analysis of the Squid Ink Polysaccharide

SE-1 (5 mg) was thoroughly hydrolyzed using 2 mol/L trifluoroacetic acid (TFA, 1 mL) at 105 °C for 6 h. The hydrolyzed product was obtained after the repetitive co-evaporation with methanol to remove TFA and derivatized with 1-phenyl-3-methyl-5-pyrazolone (PMP). The pre-column derivate was detected on an Agilent HPLC system equipped with an Agilent XDB-C18 column (4.6 mm×250 mm) and an Agilent XDB UV detector (Chen *et al*., 2011, 2012).

2.5 Atomic Force Microscopy and Infrared Spectral Analyses

SE-1 solution was dripped onto the mica substrate and dried overnight at room temperature. An image of squid ink polysaccharide was obtained by atomic force microscopy (AFM, MA-tek, Japan).

The dried polysaccharide was mixed with KBr powder and ground, then pressed into 1 mm pellets. The sample was put into an infrared spectrometer to conduct the infrared spectra at a wavelength of 4000–400 cm^{-1} for analysis.

2.6 Partial Acid Hydrolysis of the Squid Ink Polysaccharide

The polysaccharide was hydrolyzed in 0.05 mol/L trifluoroacetic acid (TFA) at 110 °C for 2 h. To remove the TFA, alcohol precipitation was carried out. The resulting supernatant was collected, concentrated, and subsequently dried. This sample was then analyzed for monosaccharide composition. For further investigation, 0.1 mol/L TFA was added to the precipitate, and the process was repeated using different concentrations of TFA (0.05, 0.1, 0.5, and 1 mol/L). Ultimately, the obtained precipitate was analyzed to determine the main and side chain components of the polysaccharides.

2.7 Methylation Analysis of the Squid Ink Polysaccharide

The modified Hakomori method was used for methylation analysis (Hakomori, 1964). Briefly, the dry sample was fully dissolved in DMSO, NaH was added quickly, and the reaction was carried out under the protection of N_2 for 1 h. Subsequently, the reaction was continued by adding CH_3I for another 1 h. The product obtained from the reaction was extracted by CH_2Cl_2 to eliminate the water-soluble impurities. The extract was dried to obtain the methylated polysaccharide. Afterward, the methylated polysaccharide was hydrolyzed, reduced, and acetylated. Ultimately, gas chromatography-mass spectrometry (GC-MS) was performed (Chen *et al*., 2011).

2.8 Nuclear Magnetic Resonance (NMR) Analysis of the Squid Ink Polysaccharide

Freeze-dried SE-1 (50 mg) was dissolved in 400 μL D_2O (99.96% atoms), and was freeze-dried twice. So the active hydrogens in the polysaccharide were replaced by the deuterium. The ^{1}H-NMR, ^{13}C-NMR, the two-dimensional ^{1}H-^{1}H COSY, ^{1}H-^{1}H NOESY, ^{1}H-^{1}H TOCSY, ^{1}H-^{13}C HMBC and ^{1}H-^{13}C HSQC spectra were recorded using a Bruker 800-MHz spectrometer (Bruker) at 25 °C. The ^{1}H and ^{13}C were fixed at 2.225 and 31.07 ppm ($\times10^{-6}$) using deuterated acetone as internal standard, respectively (Chen *et al*., 2011).

3 Results

3.1 Isolation and Purification of Squid Ink Glycosaminoglycans

The squid ink polysaccharide was initially eluted using a NaCl solution with linear concentrations ranging from 0 to 2 mol/L. Based on elution results, an appropriate concentration was selected for gradient elution, as illustrated in Fig.1. From the gradient elution curve, NaCl solutions at concentrations of 0.05, 0.25, and 0.50 mol/L were used to separate these components, which were designated SE-1, SE-2, and SE-3 respectively. Each component was collected individually and subjected to concentration processes before being dialyzed and freeze-dried for further analysis. The three fractions exhibited similar monosaccharide compositions and ratios, all of which were rich in amino sugars, uronic acids, and fucose. SE-2 and SE-3 contain over 10% protein, while SE-3 contains an even higher protein content. This may be attributed to the inherent characteristics of squid ink polysaccharides, which were originally proteoglycan structures. Incomplete enzymatic digestion might result in SE-2 and SE-3 with peptide chains covalently linked to polysaccharides. To avoid the interference of proteins in polysaccharide structure analysis, SE-1 component was chosen for further study.

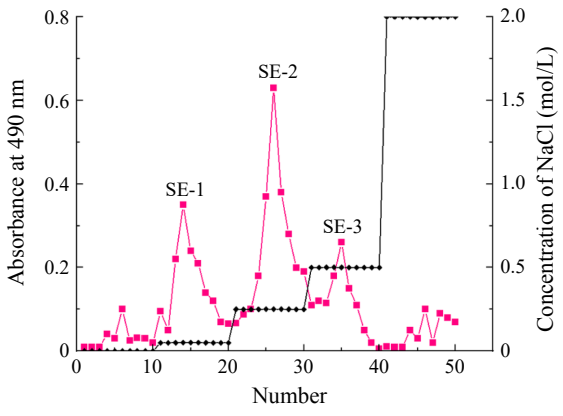

Fig.1 Segment elution of the crude *Sepia esculenta* polysaccharides.

3.2 Properties Analysis and Molecular Weight Determination of the Polysaccharide

The physicochemical properties of polysaccharides play a crucial role in further studies aimed at screening for biological activity and structural identification. We analyzed the physicochemical properties of the purified fraction SE-1. The total sugar content of SE-1 was found to be 56.2%, with a protein content of 4% and an aminosugar content of 37.1%. Additionally, the glucuronic acid content was approximately 7.5%.

The HPGPC helped to assess the purity of the polysaccharide based on the peak shape. As shown in Fig.2, the chromatogram of SE-1 showed a relatively single and symmetrical peak, indicating that the polysaccharide had high purity. According to the standard curve, the molecular weight of SE-1 was 13.1 kDa.

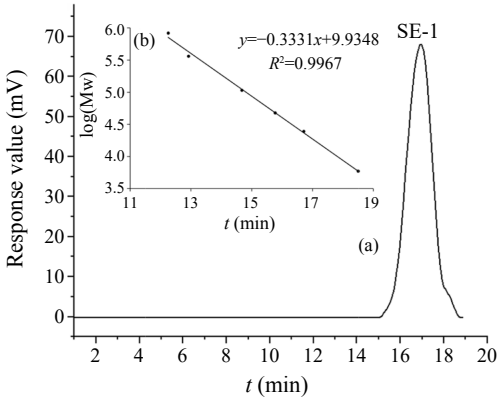

Fig.2 HPGPC chromatogram of SE-1.

3.3 Analysis of Monosaccharide Composition

The results of HPLC analyses revealed that the monosaccharide composition and ratios of the polysaccharide SE-1 were as follows: Man:GlcN:GlcUA:GalN:Xyl:Fuc= 1.00:1.38:0.65:2.89:0.76:1.99 (Fig.3). This composition indicated that the polysaccharide SE-1 derived from *Sepia esculenta* ink was a novel polysaccharide with a unique profile. Notably, it was predominantly composed of two amino sugars, GlcN and GalN, and GalN was the major component. In addition to these amino sugars, the polysaccharide also contained a small amount of uronic acid (GlcUA). The coexistence of both amino sugars and uronic acid is a typical characteristic of glycosaminoglycans.

Furthermore, SE-1 was distinguished by a significant presence of fucose, a hallmark of marine polysaccharides. It is commonly found in various marine organisms, including sea cucumbers and sea squirts. The presence of mannose and xylose in SE-1 highlighted the structural complexity of the polysaccharide derived from squid ink. While it was hypothesized that both GlcN and GalN may contain acetyl groups, as complete acid hydrolysis removes these groups.

The composition of squid ink polysaccharides varied significantly among different species. For instance, polysaccharides extracted from the ink of *Ommastrephes bartrami* predominantly consisted of three monosaccharides GlcUA, GalN, and Fuc in nearly equimolar ratios (Ye *et al*., 2019). Conversely, squid ink polysaccharides obtained from *Sepiella maindroni* were primarily composed of fucose, N-acetylgalactosamine (GalNAc), mannose, and GlcUA, with molar ratios of 2:2:1:1 (Liu *et al*., 2008). While the composition of polysaccharides SE-1 and those from *Sepiella maindroni* exhibited some similarities, the polysaccharides from *Sepia esculenta* demonstrated greater complexity, incorporating both glucosamine and xylose.

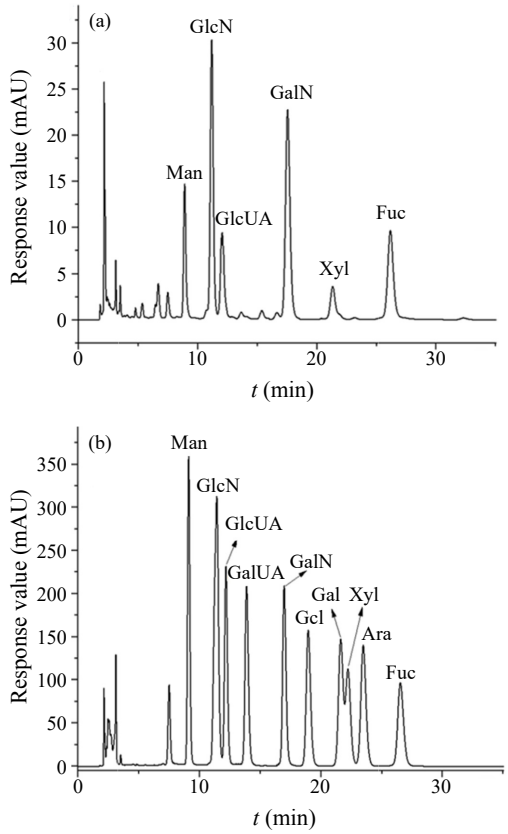

Fig.3 Analysis of monosaccharide composition. (a), HPLC chromatogram of SE-1; (b), HPLC chromatogram of standard monosaccharides.

3.4 Atomic Force Microscopy

AFM allows the visualization of polysaccharides at the nanoscale, capturing multimolecular structures under near-natural conditions. The AFM image of SE-1 was presented in Fig.4. The distribution of SE-1 was generally homogeneous, with irregular, sphere-like particles dispersed in a very dilute solution. However, the molecular chains of SE-1 exhibited variability in both shape and size, with widths ranging from a few nanometers to several tens of nanometers. In contrast, natural polysaccharide chains typically measured between 0.1 and 1.0 nm in width, significantly smaller than those observed for SE-1. This observation suggested that multiple sugar chains were interconnected and entangled, forming the larger molecular structure observed in SE-1.

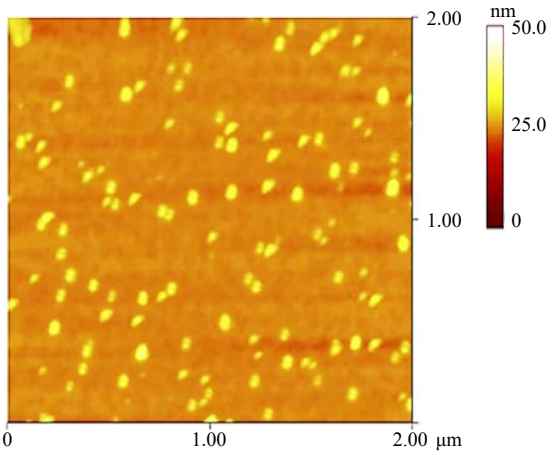

Fig.4 Atomic force microscopy of SE-1.

3.5 Partial Acid Hydrolysis

Partial acid hydrolysis is a crucial technique in polysaccharide structural analysis because different glycosidic linkages exhibit varying acid sensitivities. This selective cleavage allows researchers to determine the arrangement of monosaccharide units in the main and side chains. As SE-1 is a heteropolysaccharide with a complex structure, partial acid hydrolysis can provide essential insights into the linkage positions, branching patterns, and composition of the main and side chains. The glycosidic bonds in the main and side chains of the polysaccharides exhibited differing sensitivities to acids. Specifically, the glycosidic bonds in the side chains were less tolerant to acid than those in the main chains, making them more susceptible to hydrolysis. As illustrated in Fig.5, the concentration of Xyl decreased significantly with increasing acid concentration, while the levels of the other monosaccharides remain relatively unchanged. This observation suggests that Xyl is located in the side chains of SE-1, whereas Man, GlcN, GlcUA, GalN, and Fuc are on the main chain.

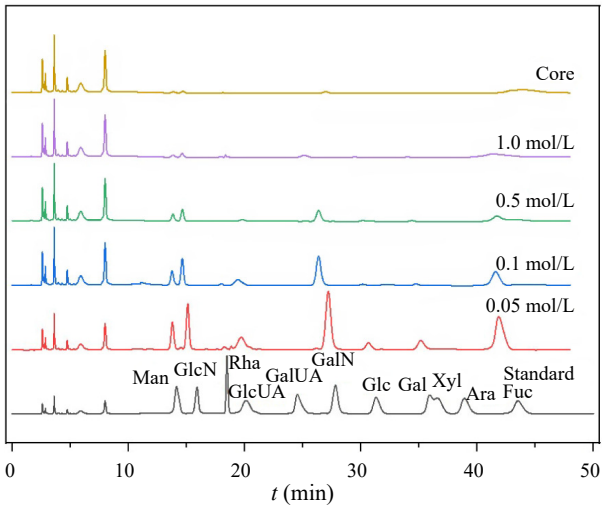

Fig.5 Partial acid hydrolysis of SE-1.

3.6 Infrared Spectral Analysis

As illustrated in Fig.6, a strong absorption peak at 3420 cm^{-1} corresponded to the characteristic vibrational bands of O-H and N-H stretching. The absorption at 2924 cm^{-1} represented the C-H stretching vibrations associated with saccharides. The relatively strong signal for methyl groups suggested that the polysaccharide may be acetylated. Additionally, the absorption at 1403 cm^{-1} was attributed to C-H bending vibrations, while the absorption at 1060 cm^{-1} indicated C-O-C stretching vibrations withintheringstructure.Notably,SE-1alsocontainedanacetylamino structure, with the peak at 1655 cm^{-1} corresponding to the C=O stretching vibration of the amide bond.

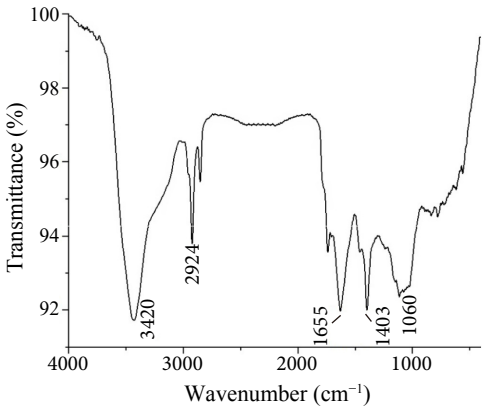

Fig.6 IR of SE-1.

3.7 Methylation Analyses

Methylation and GC-MS analyses were conducted to determine the linkages of the glycosidic bonds and further understand the structure of SE-1. Through comparing with the database of PMAA, the results were shown in Table 1. A significant quantity of 1,3,5-tri-O-acetyl-4,6-di-O-methyl-2-acetyl amino-D-galactitol confirmed the presence of →3)-Gal*p*NAc-(1→ in SE-1. Additionally, 1,4,5-tri-O-acetyl-3,6-di-O-methyl-2-acetyl amino-D-glucitol were detected, which suggested the linkage of →4)-Glc*p*NAc-(1→. The products such as 1,5-di-O-acetyl-3,4-di-O-methyl-D-xylitol and 1,4,5-tri-O-acetyl-2,3-di-O-methyl-L-fucitol indicated the presence of terminal Xyl*p*-(1→ and →4)-Fuc*p*-(1→ linkages. Moreover, the detection of 1,2,5,6-tetra-O-acetyl-3,4-di-O-methyl-D-Manni-

Table 1 GC-MS data analysis of partially O-methylated alditol acetates of SE-1

Methylated alditol acetate	MS (*m*/*z*)	Molar ratio	Linkage type
1,5-di-O-acetyl-3,4-di-O-methyl-D-xylitol	117, 129, 145, 100	1.0	Xyl*p*-(1→
1,4,5-tri-O-acetyl-2,3-di-O-methyl-L-fucitol	117, 143, 203	1.8	→4)-Fuc*p*-(1→
1,3,5-tri-O-acetyl-2,4,6-di-O-methyl-2-acetyl amino-D-galactitol	117, 129, 159, 173, 275	3.5	→3)-Gal*p*NAc-(1→
1,4,5-tri-O-acetyl-2,3,6-di-O-methyl-2-acetyl amino-D-glucitol	117, 129, 159, 233, 273	1.2	→4)-Glc*p*NAc-(1→
1,2,5,6-tetra-O-acetyl-3,4-di-O-methyl-D-mannitol	129, 189	1.1	→2,6)-Man*p*-(1→

tol indicated that SE-1 had a naturally branched linkage →2,6)-Man*p*-(1→The GC-MS analysis after methylation could not provide linkage information of uronic acids.

Based on partial acid hydrolysis data and these results, it was hypothesized that the main chain of SE-1 may consist of →4)-Fuc*p*-(1→, →4)-Glc*p*NAc-(1→, →3)-Gal*p*-NAc-(1→ with→2,6)-Man*p*-(1→ as a branch point and terminal Xyl*p*-(1→ on side chains. Due to the variety and complexity of these linkages further structural analysis is required for comprehensive characterization.

3.8 Analysis of NMR (Nuclear Magnetic Resonance) Spectroscopy

In order to accurately clarify the structure of SE-1, especially the linkage of GlcUA and linkage sequences, it was analyzed with NMR. The ^{1}H-NMR spectrum of SE-1 (Fig.7a) displayed multiple well-resolved signals in the range of δ 4.3–5.3 ppm, which were attributed to the anomeric protons of different sugar residues in the polysaccharide. The presence of distinct anomeric proton signals suggested a complex polysaccharide structure with multiple monosaccharide components. At anomeric proton region (δ 4.3–5.3 ppm), six major anomeric proton signals were observed at δ 5.21, 5.14, 5.00, 4.97, 4.38, and 4.38 ppm, which were indicative of both α- and β-configured sugar residues.

The peaks at δ 5.21, 5.14, 5.00, and 4.97 ppm suggested the presence of α-anomeric configurations, which are typically observed in glycosaminoglycan-like polysaccharides. The peaks at δ 4.38 ppm suggested β-anomeric configurations, which are characteristic of certain uronic acids and xylose residues. The anomeric carbon at the region of 95.0–105.0 ppm also confirmed both α and β configurations in SE-1 (Fig.7b) (Zhao *et al*., 2020). The signals at 1.2 and 1.8 ppm in ^{1}H NMR spectrum and signals at 15, 22 and 175 ppm in ^{13}C NMR spectrum indicated the presence of methyl and acetyl groups. The methyl group belonged to *O*-6 position of Fuc, while the acetyl groups could be the N-acetyl of Gal*p*NAc and Glc*p*NAc (Yao *et al*., 2021). From the ^{1}H-^{13}C HSQC spectrum (Fig.7e), the signal at 4.38 ppm was associated with two different anomeric carbon at 103.7 and 102 ppm respectively, which meant the anomeric protons of two different sugar residues were completely overlapped. Finally, the cross peaks at 5.21/96.9 ppm (residue **A**), 5.14/99.7 ppm (residue **B**), 5.00/99.4 ppm (residue **C**), 4.97/98.9 ppm (residue **D**), 4.38/103.7 ppm (residue **E**), and 4.38/102.0 ppm (residue **F**) were identified as the anomeric signals of six residues.

After the anomeric signals were identified, the other proton signals from H-2 to H-6 of the residues could be confirmed by ^{1}H-^{1}H COSY spectrum (Fig.7c). Due to the serious overlapping of signals in the NMR spectra, it is difficult to attribute each proton signal by ^{1}H-^{1}H COSY spectrum alone. It was necessary to combine the signals of ^{1}H-^{1}H TOCSY spectrum (Fig.7d) with the signals of ^{1}H-^{1}H COSY spectrum to determine the signals of each residue. Combined with the results of HSQC spectra, the protons and carbon atoms of individual sugar spin system are basically determined.

After determining the C/H signals of each residue, it can be found that the signals from the C4 of both **A** and **B** were shifted downfield to 78 and 80 ppm, respectively. C2 of residue **A** was shifted to 53 ppm at high field. In the ^{1}H-^{13}C HMBC spectrum (Fig.7f), the acetyl group was related to residue **A** and the methyl group was related to residue **B**. Compared with the references, it is inferred that **A** was →4)-α-Glc*p*NAc-(1→ (Peng *et al*., 2021), and **B** was →4)-α-Fuc*p*-(1→ (Yao *et al*., 2021). By analogy, it was inferred that **C** was →3)-α-Gal*p*NAc-(1→ (Chen *et al*., 2008); C2 at about 77 ppm and C6 at 68 ppm indicated residue **D** was →2,6)-α-Man*p*-(1→ (Chen *et al*., 2012). Residue **E** and **F** had β configuration. Compared with references, **E** was deduced to be terminal β-Xyl*p*-(1→ (Dubois *et al*., 1956) and **F** was →3)-β-Glc*p*UA-(1→ (Cao *et al*., 2019). The signal attribution of each residue was shown in Table 2.

By combining the ^{1}H-^{13}C HMBC spectrum (Fig.7f) and the ^{1}H-^{1}H NOESY spectrum (Fig.7g), the linkage information between the different sugar groups of SE-1 could be obtained. H-1 of **A** was associated with H-3 of **C**, suggesting that →4)-α-Glc*p*NAc-(1→ was linked to →3)-α-Gal*p*NAc(1→. H-1 of **B** was associated with H-3 and C-3 of **F** in addition to its own H-2 and C-5, indicating →4)-α-Fuc*p*-(1→ was linked to →3)-β-Glc*p*UA-(1→. H-1 of **C** was associated with H-6 and C-6 of **D** in addition to its own H-2 and C-3, indicating →3)-α-Gal*p*NAc-(1→ was linked to →2,6)-α-Man*p*-(1→ at *O*-6 position. H-1 of **D** was associated with H-4 of **B**, indicating →2,6)-α-Man*p*-(1→ linked to →4)-α-Fuc*p*-(1→ at *O*- 4. H-1 of **E** was associated with H-2 of **D**, indicating that β-Xyl*p*-(1→ was linked to →2,6)-α-Man*p*-(1→ at *O*-2. H-1 of **F** was correlated to C-4 of **B**, suggesting →3)-β-Glc*p*UA-(1→ was also connected to →4)-α-Fuc*p*-(1→. Based on all of the above chemical and spectroscopic findings, the structure of the polysaccharide SE-1 repeat unit was shown in Fig.8. SE-1 was a slightly branched heteropolysaccharide containing both amino sugar and uronic acid. The main chain of SE-1 mainly consisted of →4)-α-D-Glc*p*NAc-(1→ and →3)-α-D-Gal*p*NAc-(1→, →4)-α-D-Fuc*p*-(1→, →6)-α-D-Man*p*-(1→ and →3)-β-D-Glc*p*UA-(1→ also existed in the main chain. The branch point occurred at *O*-2 position of →6)-α-D-Man*p*-(1→ and substituted by single terminal β-D-Xyl*p*-(1→ as the side chain.

The structural characterization of the squid ink polysaccharide SE-1 revealed its unique composition and glycosidic linkages, distinguishing it from previously reported squid ink polysaccharides. Unlike glycosaminoglycans extracted from other cephalopod species, SE-1 contained both GlcNAc and GalNAc as major components, along with Fuc and GlcUA in the backbone. The presence of Man as a branch point and a terminal Xyl residue suggested a structurally complex and functionally diverse polysaccharide.

Many of the polysaccharides derived from squid ink exhibited a structure characterized by Fuc and GlcUA as the main chain, with GalN in the side chain (Ye *et al*.,

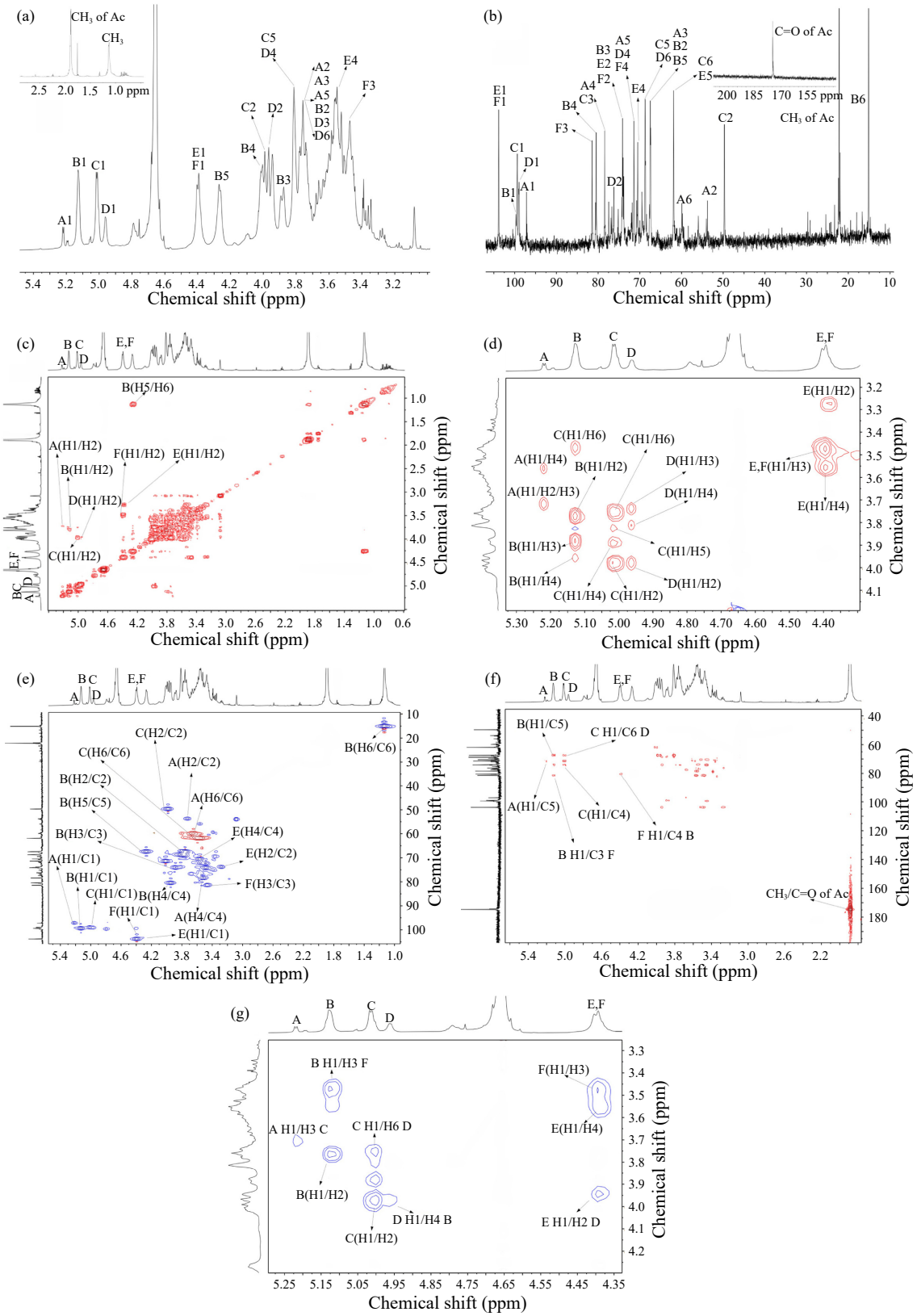

Fig.7 NMR spectra of SE-1. (a), ^{1}H NMR spectrum; (b), ^{13}C NMR spectrum; (c), ^{1}H-^{1}H COSY spectrum; (d), ^{1}H-^{1}H TOCSY spectrum; (e), ^{1}H-^{13}C HSQC spectrum; (f), ^{1}H-^{13}C HMBC spectrum; (g), ^{1}H-^{1}H NOESY spectrum.

2019). However, the polysaccharide SE-1 was more complex and resembled the glycosaminoglycan-like sugars found in *Sepiella maindroni* ink. The main chain of SE-1 comprised the following units: →4)-α-Glc*p*NAc-(1→, →4)-α-Fuc*p*-(1→, →3)-α-Gal*p*NAc-(1→, →2,6)-α-Man*p*-(1→, and →3)-β-Glc*p*UA-(1→, with a branched chain of β-Xyl*p*-(1→. In contrast, the polysaccharide from *S. maindroni* ink consists of Man with 1,6 linage and a branch at *O*-3 position, while SE-1 consists of Man at the 1,6 positions with a branch at *O*-2. Additionally, the branch in the *S. maindroni* ink polysaccharide was GlcUA, whereas it was Xyl in SE-1. Furthermore, the polysaccharide from *S.*

Table 2 ^{1}H and ^{13}C NMR chemical shifts of SE-1

Sugar residues	$^{1}H/^{13}C$ chemical shifts						
	H1/C1	H2/C2	H3/C3	H4/C4	H5/C5	H6/C6	Ac
A	5.21	3.72	3.74	3.56	3.74	3.65	1.87/22
→4)-α-D-Glc*p*NAc-(1→	96.9	53.4	67.0	78.0	71.0	59.0	175
B	5.14	3.77	3.89	3.96	4.27	1.12	
→4)-α-L-Fuc*p*-(1→	99.7	67.6	74.0	80.2	67.2	15.3	
C	5.00	3.98	3.68	3.88	3.82	3.57/3.74	1.87/22
→3)-α-D-Gal*p*NAc-(1→	99.4	50.0	78.0	73.0	68.7	61.9	175
D	4.97	3.95	3.74	3.82	3.66	3.75	
→2,6)-α-D-Man*p*-(1→	98.9	76.7	70.4	70.8	72.4	68.0	
E	4.38	3.25	3.46	3.55	3.85		
β-D-Xyl*p*-(1→	103.7	74.0	75.0	70.7	62.0		
F	4.38	3.50	3.48	3.60	3.94	–	
→3)-β-D-Glc*p*UA-(1→	102.0	74.0	81.4	70.9	–	174	

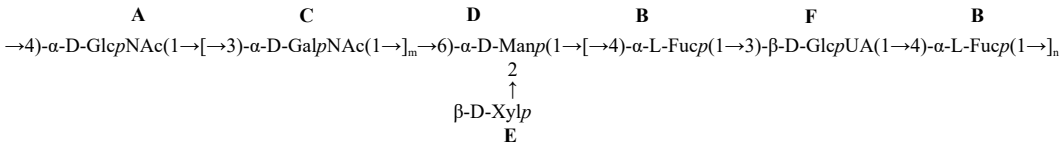

Fig.8 Proposed structure of SE-1.

maindroni ink primarily contained GalNAc, whereas SE-1 had both GlcNAc and GalNAc, with GlcUA also present in the main chain (Liu *et al*., 2008).

The physicochemical properties and glycosyl composition of SE-1 suggest its similarity to glycosaminoglycan-like structures, which have been widely studied for their bioactivities, including anticoagulant, antioxidant, and immunomodulatory effects. Previous research has demonstrated that sulfated squid ink polysaccharides can inhibit tumor growth by interfering with key signaling pathways such as EGFR/PI3K/Akt/mTOR. Given the structural similarities of SE-1 to these bioactive polysaccharides, further research should focus on its biological functionality, particularly in antitumor and immune-regulatory applications.

Furthermore, the high content of aminosugars in SE-1 suggests that it may play a role in cellular interactions and signaling. Aminosugar-rich polysaccharides have shown to influence cell adhesion, proliferation, and differentiation, making SE-1 a promising candidate for biomedical applications. Additionally, the presence of uronic acids and fucose may contribute to its potential as an anticoagulant, as similar polysaccharides have been reported to enhance blood anticoagulation properties through antithrombin activation. Further study is needed to investigate the biological activity of SE-1. This study showed that an aminosugar-abundant heteropolysaccharide was firstly obtained from *Sepia esculenta* ink.

4 Conclusions

A glycosaminoglycan-like heteropolysaccharide, designated SE-1, was successfully isolated from the ink of *Sepia esculenta*. Through monosaccharide composition analysis, partial acid hydrolysis, mass spectrometry, and nuclear magnetic resonance studies, it was determined that SE-1 comprised (1→4)-α-D-Glc*p*NAc, (1→4)-α-L-Fuc*p*, (1→3)-α-D-Gal*p*NAc, (1→2,6)-α-D-Man*p* and (1→3)-β-D-Glc*p*UA as the main chain. Additionally, a side chain of terminal β-D-Xyl*p*-(1→ was attached to *O*-2 of the →2,6)-α-Manp-(1→ residue in the main chain.

Acknowledgements

This work was funded by the Natural Science Foundation of Zhejiang Province, China (No. LTGS23D060001), and the Scientific Research Foundation for the Introduction of Talent of Zhejiang Ocean University (No. JX631 1130823).

Author Contributions

Cheng Ji: data curation and analysis, original draft preparation. Zefeng Xia and Chunyu Niu: methodology and data analysis on bioactivity. Yin Chen: analysis on NMR and sample preparation. Yan Chen, Jinfeng Pei and Yin Chen: conceptualization, funding acquisition, project administration, article reviewing.

Data Availability

All data generated during this study are presented in this published article, and are also available from the corresponding authors upon reasonable request.

Declarations

Ethics Approval and Consent to Participate

This article does not contain any studies with human

participants or animals performed by the authors.

Consent for Publication

Informed consent for publication was obtained from all participants.

Conflict of Interest

All authors declare that they have no conflict of interest in publishing this paper.

References

Cao, J., Lv, Q., Zhang, B., and Chen, H., 2019. Structural characterization and hepatoprotective activities of polysaccharides from the leaves of *Toona sinensis* (A. Juss) Roem. *Carbohydrate Polymers*, **212**: 89–101.

Chen, S., Xu, J., Xue, C., Dong, P., Sheng, W., Yu, G., *et al*., 2008. Sequence determination of a non-sulfated glycosaminoglycan-like polysaccharide from melanin-free ink of the squid *Ommastrephes bartrami* by negative-ion electrospray tandem mass spectrometry and NMR spectroscopy. *Glycoconjugate Journal*, **25**: 481–492.

Chen, Y., Mao, W., Tao, H., Zhu, W., Qi, X., Chen, Y., *et al*., 2011. Structural characterization and antioxidant properties of an exopolysaccharide produced by the mangrove endophytic fungus *Aspergillus* sp. Y16. *Bioresource Technology*, **102** (17): 8179–8184.

Chen, Y., Mao, W., Wang, B., Zhou, L., Gu, Q., Chen, Y., *et al*., 2013. Preparation and characterization of an extracellular polysaccharide produced by the deep-sea fungus *Penicillium griseofulvum*. *Bioresource Technology*, **132**: 178–181.

Chen, Y., Mao, W., Yang, Y., Teng, X., Zhu, W., Qi, X., *et al*., 2012. Structure and antioxidant activity of an extracellular polysaccharide from coral-associated fungus, *Aspergillus versicolor* LCJ-5-4. *Carbohydrate Polymers*, **87**: 218–226.

Clark, A. G., and Vignjevic, D. M., 2015. Modes of cancer cell invasion and the role of the microenvironment. *Current Opinion in Cell Biology*, **36**: 13–22.

Dubois, M., Gilles, K. A., Hamilton, J. K., Rebers, P. A., and Smith, F., 1956. Colorimetric method for determination of sugars and related substances. *Analytical Chemistry*, **28**: 350–356.

Gu, Y., Yang, X., Duan, Z., Luo, P., Shang, J., Xiao, W., *et al*., 2017. Inhibition of chemotherapy-induced apoptosis of testicular cells by squid ink polysaccharide. *Experimental and Therapeutic Medicine*, **14**: 5889–5895.

Hakomori, S., 1964. A rapid permethylation of glycolipid, and polysaccharide catalyzed by methylsulfinyl carbanion in dimethyl sulfoxide. *Journal of Biochemistry*, **55**: 205–208.

Hida, K., Maishi, N., Torii, C., and Hida, Y., 2016. Tumor angiogenesis-characteristics of tumor endothelial cells. *International Journal of Clinical Oncology*, **21**: 206–212.

Jeong, Y. J., Choi, Y., Shin, J. M., Cho, H. J., Kang, J. H., Park, K. K., *et al*., 2014. Melittin suppresses EGF-induced cell motility and invasion by inhibiting PI3K/Akt/mTOR signaling pathway in breast cancer cells. *Food and Chemical Toxicology*, **68**: 218–225.

Jiang, W., Cheng, Y., Zhao, N., Li, L., Shi, Y., Zong, A., *et al*., 2018. Sulfated polysaccharide of *Sepiella maindroni* ink inhibits the migration, invasion and matrix metalloproteinase-2 expression through suppressing EGFR-mediated p38/MAPK and PI3K/Akt/mTOR signaling pathways in SKOV-3 cells. *International Journal of Biological Macromolecules*, **107**: 349–362.

Jin, Y., Huang, M., Wang, Y., Yi, C., Deng, Y., Chen, Y., *et al*., 2016. c-Yes enhance tumor migration and invasion via PI3K/AKT pathway in epithelial ovarian cancer. *Experimental and Molecular Pathology*, **101**: 50–57.

Le, X., Luo, P., Gu, Y., Tao, Y., and Liu, H., 2015. Squid ink polysaccharide reduces cyclophosphamide-induced testicular damage via Nrf2/ARE activation pathway in mice. *Iranian Journal of Basic Medical Sciences*, **18**: 827–831.

Li, F., Lin, Z., Wu, Y., Luo, P., Wu, J., and Liu, H., 2022. Antioxidant, anticoagulant and thrombolytic properties of SIP-IV, a sulfated polysaccharide from *Sepia esculenta* ink, and its derivatives. *Food Bioscience*, **49**: 101959.

Li, F., Luo, P., and Liu, H., 2018. A potential adjuvant agent of chemotherapy: Sepia ink polysaccharides. *Marine Drugs*, **16**: 106.

Li, X., Wang, F., Song, Y., Cao, J., and Xu, B., 2004. Study on the preparation and properties of glycosaminoglycans from the ink of *Sepiella maindroni* de Rochebrune. *Chinese Journal of Marine Drugs*, **23**: 24–27.

Liu, B., Gu, X., Wang, B., and Chu, M., 2023. Visualization of cephalopod beak pigmentation and its application to the classification of cephalopods. *Journal of Shanghai Ocean University*, **32**: 785–793.

Liu, C., Li, X., Li, Y., Feng, Y., Zhou, S., and Wang, F., 2008. Structural characterisation and antimutagenic activity of a novel polysaccharide isolated from *Sepiella maindroni* ink. *Food Chemistry*, **110**: 807–813.

Liu, Z., Wu, M., Fang, X., Yang, J., Chen, Q., and Chen, X., 2022. Extraction optimization, characterization, antioxidant and immunological activities of polysaccharides from squid (*Ommastrephes bartramii*) viscera. *Journal of Food Measurement and Characterization*, **16**: 4615–4629.

Lowry, O. H., Rosebrough, N. J., Farr, A. L., and Randall, R. J., 1951. Protein measurement with the Folin phenol reagent. *The Journal of Biological Chemistry*, **193**: 265–275.

Luo, P., and Liu, H., 2013. Antioxidant ability of squid ink polysaccharides as well as their protective effects on deoxyribonucleic acid DNA damage *in vitro*. *African Journal of Pharmacy and Pharmacology*, **7**: 1382–1388.

Patan, S., 2014. ERBB1/EGFR and ERBB2 (HER2/neu)-targeted therapies in cancer and cardiovascular system with cardiovascular drugs. *International Journal of Cardiology*, **176**: 1301–1303.

Peng, D., Wen, Y., Bi, S., Huang, C., Yang, J., Guo, Z., *et al*., 2021. A new GlcNAc-containing polysaccharide from *Morchella importuna* fruiting bodies: Structural characterization and immunomodulatory activities *in vitro* and *in vivo*. *International Journal of Biological Macromolecules*, **192**: 1134–1149.

Reissig, J. L., Storminger, J. L., and Leloir, L. F., 1955. A modified colorimetric method for the estimation of N-acetylamino sugars. *The Journal of Biological Chemistry*, **217**: 959–966.

Schmitt, J., and Matei, D., 2012. Targeting angiogenesis in ovarian cancer. *Cancer Treatment Reviews*, **38**: 272–283.

Shi, L., Liu, H., Zhong, J., and Pan, J., 2015. Fresh-keeping effects of melanin-free extract from squid ink on yellowfin sea bream (*Sparus latus*) during cold storage. *Journal of Aquatic Food Product Technology*, **24**: 199–212.

Takaya, Y., Uchisawa, H., Matsue, H., Okuzaki, B., Narumi, F., Sasaki, J., *et al*., 1994. An investigation of the antitumor peptidoglycan fraction from squid ink. *Biological & Pharmaceutical Bulletin*, **17**: 846–849.

Takaya, Y., Uchisawa, H., Narumi, F., and Matsue, H., 1996. Illexins A, B, and C from squid ink should have a branched structure. *Biochemical and Biophysical Research Communications*, **226**: 335–338.

Tian, W., Song, X., Wang, F., and Jiang, W., 2023. Study on the preparation and biological activities of low molecular weight squid ink polysaccharide from *Sepiella maindroni*. *International Journal of Biological Macromolecules*, **237**: 124040.

Yao, H., Wang, J., Yin, J., Nie, S., and Xie, M., 2021. A review of NMR analysis in polysaccharide structure and conformation: Progress, challenge and perspective. *Food Research International*, **143**: 110290.

Ye, P., Li, P., Yang, W., Zhao, Y., Zhao, Y., Sun, K., *et al*., 2019. Structure and neuroprotective effect of polysaccharide from viscera autolysates of squid *Ommastrephes bartrami*. *Marine Drugs*, **17**: 188.

Zhang, X., Liu, T., Guo, X., and Yin, X., 2013. The determination of protein content in tea. *Journal of Anhui Agricultural Sciences*, **41**: 9058–9059.

Zhang, X., Ruan, Y., Li, Y., Lin, D., and Quan, C., 2015. Tight junction protein claudin-6 inhibits growth and induces the apoptosis of cervical carcinoma cells *in vitro* and *in vivo*. *Medical Oncology*, **32**: 148.

Zhao, K., Li, B., He, D., Zhao, C., Shi, Z., Dong, B., *et al*., 2020. Chemical characteristic and bioactivity of hemicellulose-based polysaccharides isolated from *Salvia miltiorrhiza*. *International Journal of Biological Macromolecules*, **165**: 2475–2483.

Zong, A., Zhao, T., Zhang, Y., Song, X., Shi, Y., Cao, H., *et al*., 2013. Anti-metastatic and anti-angiogenic activities of sulfated polysaccharide of *Sepiella maindroni* ink. *Carbohydrate Polymers*, **91**: 403–409.

Zuo, T., Cao, L., Li, X., Zhang, Q., Xue, C., and Tang, Q., 2015. The squid ink polysaccharides protect tight junctions and adherens junctions from chemotherapeutic injury in the small intestinal epithelium of mice. *Nutrition and Cancer*, **67**: 364–371.

(Edited by Qiu Yantao)